# Natural Products for Materials Protection: Corrosion and Microbial Growth Inhibition Using *Capsicum frutescens* Biomass Extracts

Emeka E. Oguzie,*,[†] Kanayo L. Oguzie,[‡] Chris O. Akalezi,[†] Irene O. Udeze,[§] Jude N. Ogbulie,[§] and Victor O. Njoku[||]

[†]Electrochemistry and Material Science Research Laboratory, Department of Chemistry, Federal University of Technology Owerri, PMB 1526, Owerri, Nigeria

[‡]Department of Environmental Technology and [§]Department of Microbiology, Federal University of Technology, PMB 1526, Owerri, Nigeria

[||]Department of Chemistry, Imo State University Owerri, PMB 2000, Owerri. Nigeria
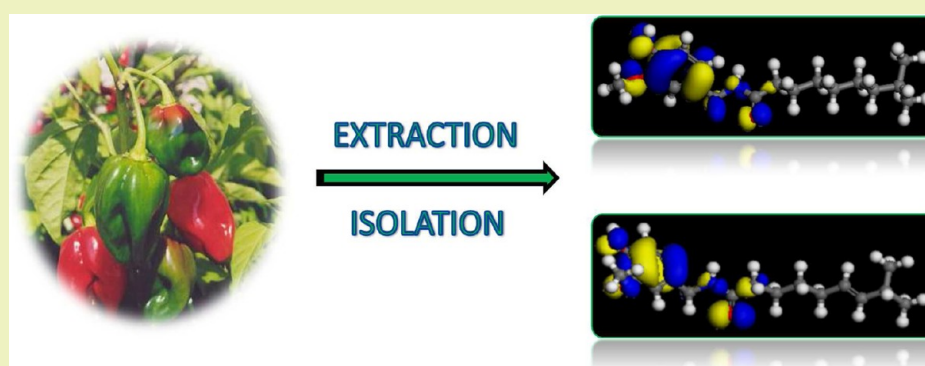
ABSTRACT: Extracts of the fruit of *Capsicum frutescens* (CF) were assessed for anticorrosion and antimicrobial activity. The anticorrosion effect of the ethanol extract on low carbon steel in acidic media was studied experimentally using gravimetric, impedance, and polarization techniques, while the antimicrobial efficacy of ethanol, methanol, water, and petroleum spirit extracts respectively against the corrosion-associated sulfate reducing bacteria (SRB), *Desulfotomaculum* species, was assessed using the agar disc diffusion method. CF extract effectively inhibited both corrosion and SRB growth due to the action of the phytochemical constituents present therein, including alkaloids (8.8%), tannins (0.4%), and saponins (39.2%). The corrosion process was inhibited by adsorption of the extract organic matter on the steel surface, whereas the antimicrobial effect results from disruption of the growth and essential metabolic functions of the SRB. Molecular dynamics (MD) simulations were performed to theoretically illustrate the electronic structure and adsorption behavior of the active alkaloidal constituents of CF extract, capsaicin and dihydrocapsaicin, and afforded molecular level insights on their individual contributions to the corrosion inhibiting action of the extract.

KEYWORDS: *Low carbon steel, Biomass extracts, Corrosion inhibition, Antimicrobial activity, Adsorption*

INTRODUCTION

Corrosion of iron and steel surfaces deployed in service in aqueous acidic environments often leads to enormous economic losses as well as safety hazards since catastrophic failures resulting from the corrosion of engineering structures are well-known. A significant method to protect the metals from corrosion is by addition of species to the solution in contact with the surface in order to inhibit the corrosion reaction and reduce the corrosion rate. To this end, the use of organic compounds containing nitrogen, oxygen, and/or sulfur in a conjugated system as inhibitors to reduce corrosion attack has received detailed attention.[1−10] These compounds act at the interphase created by corrosion product between the metal and aqueous aggressive solution and their interaction with the corroding metal surface, usually via adsorption, often leads to a modification in either the mechanism of the electrochemical process at the double layer or in the surface available to the process.

Microbial slime layers, known as biofilms, form over a period of days on metal surfaces exposed to aqueous environments such as soil sediments, oil fields, fuels, and lubrication systems.[11−15] The biofilms influence interactions between metal surfaces and the environment by altering the electrochemical conditions at the metal/solution interface. It is estimated that microbial influenced corrosion (MIC) accounts for nearly 50% of the total cost of corrosion.[16] Corrosion processes under the biofilms depend on the film constitution, irregularity of the surface coverage, or the local metabolic effects of the microbial consortium, which may manifest in

stimulation of localized corrosion, acceleration of the rate of uniform corrosion, or even corrosion inhibition.[12] Chemicals that control microbial activity are called biocides. Such biocides, which include formaldehyde, glutaraldehyde, isothiazolones, and quaternary ammonia compounds are capable of killing or inhibiting the growth and/or metabolic activity of micro-organisms.[13]

Due to increasing ecological awareness and strict environmental regulations, the surface coatings industry is being challenged by an ever-increasing number of regulatory initiatives designed to protect the environment and workforce from harmful effects of corrosion and scale inhibitors as well as biocides used as coating additives. Most obvious among these are restrictions on hazardous air pollutants (HAP) and volatile organic content (VOC) as well as increasing pressure and restrictions on heavy metals. Some heavy metal-based corrosion inhibitors cause profound damage to the body tissue. Cr(VI) for instance is a highly toxic carcinogen and can induce ulcers and holes in the nasal septum, while skin contact causes skin ulcers and could be quite fatal if ingested in large doses. Cr(VI) is considered a pollutant in the environment because it is quite soluble and readily leached from soils to contaminate surface and subsurface waters.[17,18]

The ideal approach to reduce the adverse effect of such hazardous materials is substitution with less toxic alternatives. In this regard, there has been growing interest in the exploitation of biomass extracts as readily available, low-cost, and renewable sources of corrosion inhibiting additives.[19−26] Such interest is justified by the phytochemical constituents of the extracts, which often bear similar molecular and electronic structures with conventional organic corrosion inhibitors; (i.e., the presence of electronegative atoms (N, O, S), aromatic rings, extensive conjugation, and a high degree of planarity), which give them the ability to attach to corroding metal surfaces. In addition, the use of biomass extracts as biocides is justified by the proven antimicrobial activity of some biomass extracts on pathogenic microorganisms,[27,28] which could be further exploited for the control of corrosion−associated micro-organisms such as sulfate reducing bacteria (SRB).

In the present study, the inhibiting effect of ethanol extracts of *Capsicum frutescens* (bell pepper) on the acid corrosion of low carbon steel, including evaluation of the electronic and adsorption structures of key phytochemical constituents of the extract have been investigated using combined experimental and computational techniques. The antimicrobial activity of the ethanol, methanol, petroleum spirit, and water extracts, respectively, on the corrosion-associated SRB (*Desulfotomaculum*) species was also assessed. Fruits of bell pepper like other pepper fruits have been used since ancient times as food flavor and in traditional medicine. Corrosion rates were experimentally evaluated using weight loss, electrochemical impedance, and potentiodynamic polarization measurements, while computations were performed within the framework of the density functional theory (DFT), to theoretically ascertain the possible adsorption energies of selected constituents. Antimicrobial screening to determine the growth inhibition of the extract against the SRB was by the agar disc diffusion method. The minimum inhibitory concentration was assessed using the serial dilution method.

EXPERIMENTAL SECTION

Materials Preparation. *Metal Specimen.* Corrosion experiments were performed on low carbon steel specimens with weight percentage composition as follows; C 0.05; Mn 0.6; P 0.36; Si 0.3 and balance Fe. The aggressive solutions were respectively 1.0 M HCl and 0.5 M H_2SO_4 prepared from analytical grade reagents (JHD China).

Biomass Extract. Corrosion Inhibition Tests. The stock solution of the biomass extract for corrosion inhibition studies was prepared by boiling weighed amounts of the dried and ground fruits of *Capsicum frutescens* (CF) in ethanol under reflux for 3 h. The resulting solution was cooled and then triple filtered. The amount of plant material extracted into solution was quantified by comparing the weight of the dried residue with the initial weight of the dried plant material before extraction. From the respective stock solutions, inhibitor test solutions were prepared in the desired concentration range by diluting with the respective aggressive solutions.

Phytochemical screening to detect the presence and relative amounts of alkaloids, saponins, and tannins in the CF extract was undertaken using standard laboratory procedures.[29]

Antimicrobial Tests. In order to prepare the extracts for antimicrobial experiments, the dried and ground CF biomass was extracted separately with ethanol (cold and hot), methanol (cold and hot), petroleum spirit and water (cold and hot). Extraction was by Soxhlet and decoction methods and lasted for 3 h. The solvents after filtration were removed in a rotary evaporator.

The sulfate reducing bacteria (*Desulfotomaculum* species) was obtained from corroded pipeline steel specimens collected from the facilities of an oil and gas company. The rust layer was scrapped and diluted (10-fold serial dilutions) with distilled water, 1 mL of the fifth serial dilution was collected and inoculated in Postgate and Baar's media and incubated in an anaerobic jar with gas park at room temperature for 14 days. Microbial colonies were isolated and characterized in sterile nutrient agar media and the *Desulfotomaculum* species identified by gram staining and positive response to oxidase, citrate, and mannose tests, based on the sulfate-reducing and spore-forming properties of *Desulfotomaculum* species.

Gravimetric Experiments. Gravimetric experiments were conducted on test coupons of dimension 3 cm × 3 cm × 0.14 cm. These coupons were wet-polished with silicon carbide abrasive paper (from grade no. 400 to 1000), rinsed with distilled water, dried in acetone and warm air, weighed, and stored in moisture-free desiccators prior to use. The precleaned and weighed coupons were suspended in beakers containing the test solutions using glass hooks and rods. Tests were conducted under total immersion conditions in 300 mL of the aerated and unstirred test solutions. To determine weight loss with respect to time, the coupons were retrieved at 24 h intervals progressively for 144 h, immersed in 20% NaOH solution containing 200 g/L of zinc dust, scrubbed with bristle brush, washed, dried, and weighed. The weight loss was taken to be the difference between the weight of the coupons at a given time and its initial weight. All tests were run in triplicate, and the data showed good reproducibility. Average values for each experiment were obtained and used in subsequent calculations.

The effect of temperature on the corrosion and corrosion inhibition processes was investigated by carrying out gravimetric experiments in the temperature range 303−333 K.

Electrochemical Measurements. Metal samples for electrochemical experiments were machined into test electrodes of dimension 1 cm × 1 cm and fixed in polytetrafluoroethylene (PTFE) rods by epoxy resin in such a way that only one surface, of area 1 cm^2, was left uncovered. The exposed surface was cleaned using the procedure described above. Electrochemical experiments were conducted in a conventional three-electrode glass cell of capacity 400 mL using a VERSASTAT 3 Complete DC Voltammetry and Corrosion System, with V3 Studio software. A graphite rod was used as counter electrode, and a saturated calomel electrode (SCE) was used as reference electrode. The latter was connected via a Luggin's capillary. Measurements were performed in naturally aerated and unstirred solutions at the end of 1 h of immersion at 303 K. Impedance measurements were made at corrosion potentials (E_{corr}) over a frequency range of 100 kHz−10 mHz, with a signal amplitude perturbation of 5 mV. Potentiodynamic polarization studies were carried out in the potential range ±250 mV versus corrosion potential

at 0.333 mV/s scan rate. Each test was run in triplicate to verify the reproducibility of the data.

Antimicrobial Screening. The CF extract was assessed for antimicrobial activity using the disc diffusion technique. About 100 g of the dried and powdered CF was extracted with 500 mL each of cold ethanol (CE), hot ethanol (HE), cold methanol (CM), hot methanol (HM), petroleum spirit (PS), cold water (CW), and hot water (HW), respectively, to yield seven distinct extracts. An overnight broth culture of the *Desulfotomaculum* species was subjected to a series of culturing, subculturing, and dilutions to obtain a standard suspension for the test. The standard suspension was inoculated anaerobically on sterile nutrient agar plates and filter paper discs impregnated with the respective extracts subsequently placed aseptically on the seeded agar plates, which were then incubated at 28 °C for 24 h. After incubation, the plates were examined for zones of growth inhibition around the disc. The radius of the zone of inhibition was measured from the edge of the disc to the edge of the zone. Similar tests were performed using 60% and 80% concentrations of the respective extracts appropriately diluted with distilled water. Triplicate determinations were undertaken for each system, and the mean values were obtained.

To determine the minimum inhibitory concentrations of the extract, the solvent in the stock extract solution was evaporated and the solid residue diluted in Baar's medium to yield seven different concentrations (3.1, 6.25, 12.5, 25, 50, 100, and 200 mg/L). About 0.9 mL was collected from each system and was added to a test tube with 0.1 mL of the standard SRB culture. The test tubes were incubated anaerobically at ambient temperature for 24 h and checked for turbidity. The lowest concentration of the extract that showed visible growth inhibition was recorded as the minimum inhibitory concentration.

Theoretical Modeling and Simulation. All theoretical calculations were performed using the density functional theory (DFT) electronic structure programs Forcite and DMol[3] as contained in the Materials Studio 4.0 software (Accelrys, Inc.).

■ RESULTS AND DISCUSSION

Preliminary Phytochemical Analysis. The results of the proximate phytochemical screening and percentage amounts of key phytochemical constituents of CF extract were as follows; alkaloids (8.8%), tannins (0.4%), and saponins (39.2%). The alkaloidal constituents responsible for the pungency and peppery flavor are collectively called capsaicinoids and include capsaicin (69%), dihydrocapsaicin (22%), nordihydrocapsaicin (7%), homodihydrocapsaicin (1%), and homocapsaicin (1%).[30,31] Figure 1 illustrates the molecular structures of the main capsaicinoids: capsaicin (Figure 1a) and dihydrocapsaicin (Figure 1b).

Gravimetric Data. *Weight Loss and Corrosion Rates.* The inhibitive effect of the ethanol extracts of *Capsicum frutescens* (CF) on the corrosion of low carbon steel in 1 M HCl and 0.5
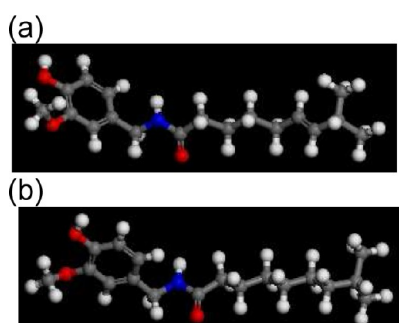
Figure 1. Molecular structures of the main capsaicinoids present in *Capsicum frutescens* (CF) extract (a) capsaicin and (b) dihydrocapsaisin. Atom legend: (white) H; (gray) C; (red) O; (blue) N.

M H₂SO₄ was investigated using a gravimetric technique. The data presented are means of triplicate determinations, with standard deviation < 0.001. Figure 2 shows the weight losses of
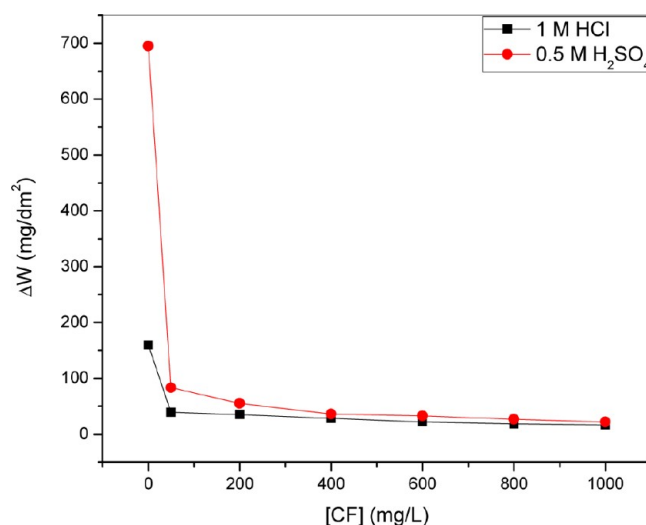
Figure 2. Weight loss of low carbon steel 1 M HCl and 0.5 M H₂SO₄ without and with different concentrations of *Capsicum frutescens* (CF) extract at 30 °C.

low carbon steel coupons in 1 M HCl and 0.5 M H₂SO₄ without and with different concentrations of CF extract. The plots show higher corrosion rates in 0.5 M H₂SO₄ and as well provide clear evidence that CF extract inhibited the corrosion reaction in the two types of acid environments, even though this effect was more pronounced in 0.5 M H₂SO₄.

Inhibition Efficiency and Surface Coverage. The efficiency of inhibition, IE (%), was quantified by comparing the weight losses of carbon steel specimens in uninhibited (ΔW_{blank}) and inhibited (ΔW_{inh}) solution as follows:

$$IE\% = \left(1 - \frac{\Delta W_{inh}}{\Delta W_{blank}}\right) \times 100 \tag{1}$$

Figure 3 illustrates the trend of inhibition efficiency values with CF concentration. The results confirm that the extract was more effective in 0.5 M H₂SO₄ at all studied concentrations.

The relationship between the degree of surface coverage, θ (related to the inhibition efficiency by IE (%) = $\theta \times 100$) and CF extract concentration (C) was adapted to determine the experimental data fit for the different acid media to the Langmuir adsorption isotherm (eq 2):

$$C/\theta = 1/b + C \tag{2}$$

The term b is a constant. The plot of C/θ vs C is shown in Figure 4 to be linear for CF extract in both 1 M HCl and 0.5 M H₂SO₄, with slopes of 1.09 and 1.03, respectively, suggesting that the experimental data follows the Langmuir isotherm. This isotherm fit of the gravimetric data suggests that the extract is adsorbed on the corroding metal surface. The deviation of the slopes of the Langmuir plots from unity can be attributed to interactions between adsorbate species on the metal surface as well as changes in the adsorption heat with increasing surface coverage.[32,33]

The complex chemical composition of biomass extracts makes it quite difficult to comprehensively discuss their adsorption characteristics. Nonetheless, it is expected that
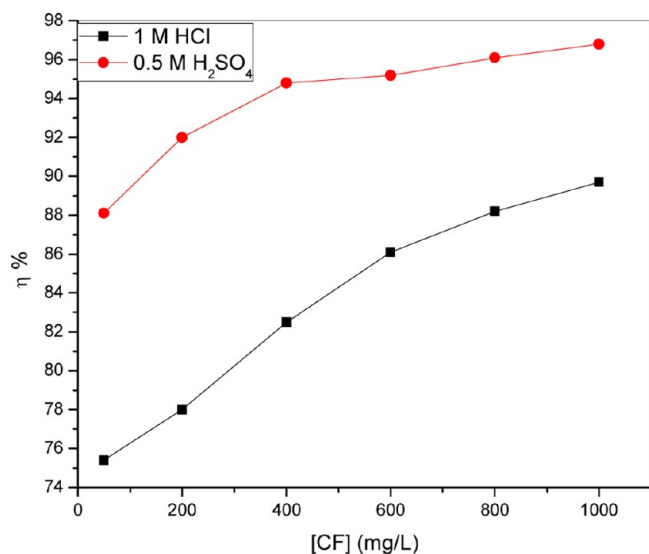
Figure 3. Trend of inhibition efficiency with concentration of CF extract for low carbon steel corrosion in 1 M HCl and 0.5 M H_2SO_4 at 30 °C.
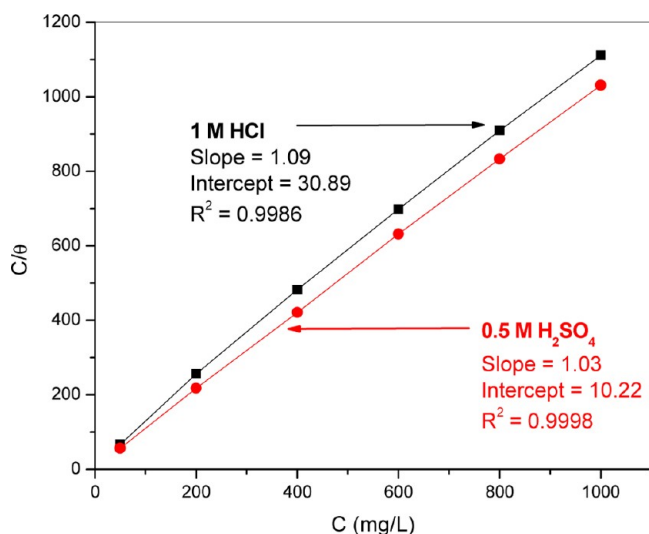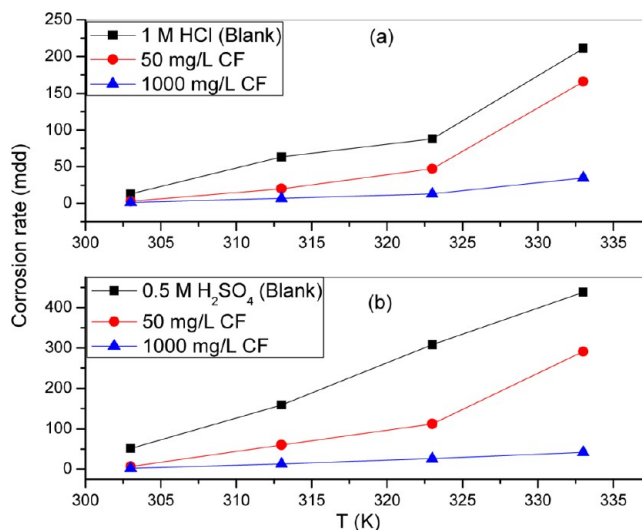

Figure 4. Langmuir adsorption isotherms for CF extract on low carbon steel in (a) 1 M HCl and (b) 0.5 M H_2SO_4 solutions.

appropriately reflect the temperature effects at low and high surface coverage. The results obtained after 3 h of immersion are presented in Figure 5 for 1 M HCl (Figure 5a) and 0.5 M

Figure 5. Effect of temperature on the corrosion rates of low carbon steel (a) 1 M HCl and (b) 0.5 M H_2SO_4 solutions without and with CF extract.

H_2SO_4 (Figure 5b) and show that corrosion rates in all systems increased with rise in temperature. CF can as well be seen to hinder the corrosion reaction in both acid media at all temperatures. Figure 6 illustrates the trend of inhibition
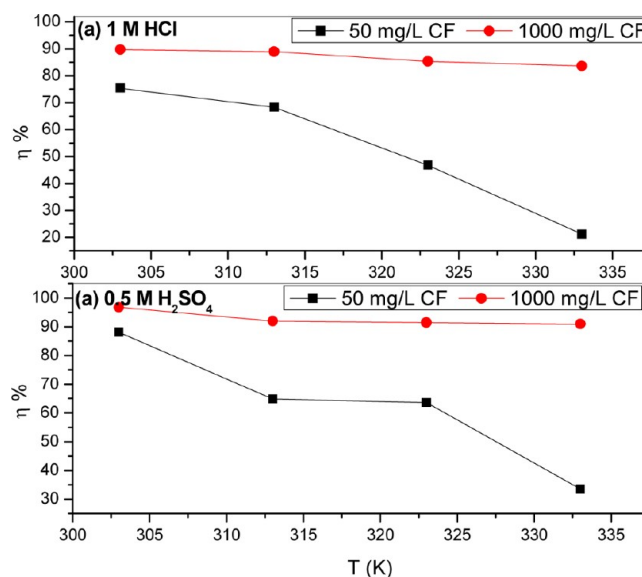
Figure 6. Relationship between inhibition efficiency of CF extracts and temperature for low carbon steel corrosion in (a) 1 M HCl and (b) 0.5 M H_2SO_4 solutions.

some of the organic constituents of the extract would be protonated in the acidic environment while some remain as unprotonated (molecular) species. Accordingly, the corrosion inhibition and adsorption behavior of CF extract under any given condition will depend on the relative involvement of both protonated and molecular species including the nature of their interaction with the metal surface.

Effect of Temperature on Corrosion and Corrosion Inhibition. Temperature has a significant influence on metal corrosion rates. When the electrochemical corrosion reaction involves a cathodic process of hydrogen depolarization (as in the present study), the corrosion rate increases exponentially with rise in temperature according to Arrhenius-type dependence. In order to evaluate the effect of temperature variation on the corrosion and corrosion inhibition processes, gravimetric tests were further undertaken at 313−333 K in both uninhibited and inhibited systems. Low (50 mg/L) and high (1000 mg/L) concentrations of CF extract were selected to
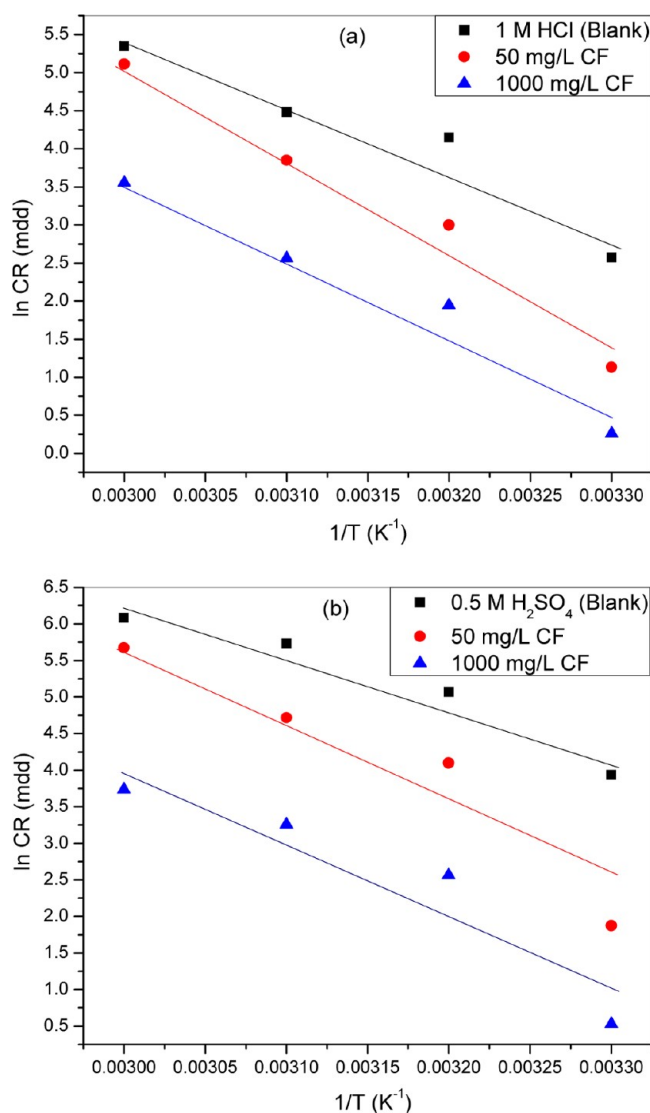
efficiency of CF extract with temperature. Inhibition efficiency in 1 M HCl and 0.5 M H_2SO_4 decreased with rise in temperature. Such decrease in inhibition efficiency, which was more pronounced at low CF concentrations, suggests that the adsorption−desorption equilibrium is shifted toward desorption with increasing temperature, indicating a physical adsorption mechanism. The physisorbed inhibitor species are often perturbed and even dispersed by the increased agitation

of the interface due to enhanced rates of hydrogen gas evolution at higher temperatures. This tends to reduce the degree of surface coverage and inhibition efficiency. Interestingly, the decrease in efficiency with rise in temperature is not so pronounced at high inhibitor concentration since the amount of inhibiting species available for adsorption is somewhat high so a relatively high degree of surface coverage is maintained even at high temperature. Again, it is possible that high extract concentrations increased involvement of chemisorbed species. Accordingly, the obtained inhibition efficiency for CF extract exceeded 80% at all temperatures.

The Arrhenius-type relationship between the corrosion rate (k) of carbon steel in acidic media and temperature (T) as often expressed by the Arrhenius equation was used to determine the activation energies (E_a):

$$k = A \exp(-E_a/RT) \tag{3}$$

A is the pre-exponential factor, and R the universal gas constant. The variation of logarithm of corrosion rate with reciprocal of absolute temperature is shown in Figure 7 for 1 M HCl and 0.5 M H_2SO_4 without and with CF extract. The calculated values of E_a are given in Table 1. Consistent with the trend of inhibition efficiency with temperature, addition of CF extract is seen to

Table 1. Corrosion Activation Energies (E_a) for Low Carbon Steel in 1 M HCl and 0.5 M H_2SO_4 without and with CF Extract

system	E_a (kJ mol^{-1})	
	1 M HCl	0.5 M H_2SO_4
blank	72.1	59.1
50 mg/L CF	106.4	100.0
1000 mg/L CF	87.3	85.8

increase E_a for the corrosion reaction in 1 M HCl and 0.5 M H_2SO_4, implying that the extract is more effective in these media at lower temperatures. It is noteworthy that E_a values in inhibited solutions decreased notably at high CF concentrations, possibly because some of the energy is gradually used up as chemisorptive interactions between some extract constituents and the metal surface scale up.
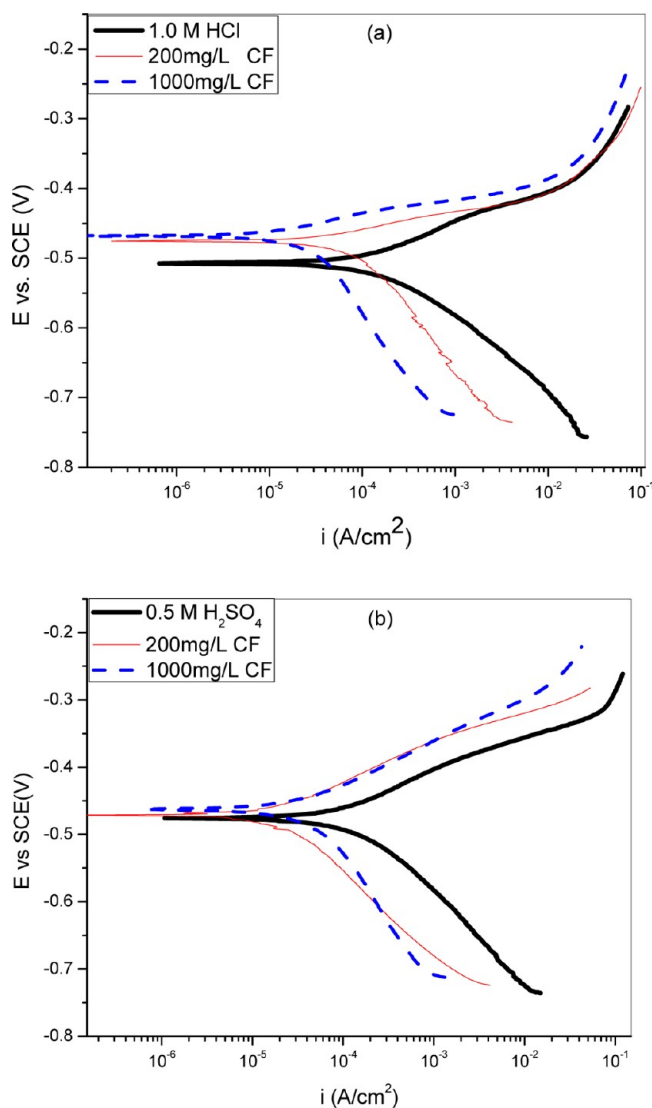
Potentiodynamic Polarization Data. Potentiodynamic polarization experiments were carried out to ascertain the influence of CF extract on the kinetics of the anodic and cathodic partial reactions of the corrosion process. Figure 8a and b depicts typical potentiodynamic polarization curves for the low carbon steel specimen in 1 M HCl and 0.5 M H_2SO_4 without and with 200 and 1000 mg/L concentrations of CF extract. The corresponding polarization parameters are presented in Table 2. The polarization curves show that CF extract inhibited both the anodic metal dissolution reaction as well as the cathodic partial reactions of the corrosion process, without notably altering the corrosion potential. This implies that the extract functioned via mixed inhibition mechanism, reducing the rates of both anodic and cathodic reactions. It can however be seen that the cathodic inhibiting effect was more dominant in 1 M HCl (Figure 8a), whereas the anodic effect becomes more pronounced in 0.5 M H_2SO_4 (Figure 8b). The anodic and cathodic inhibiting effect is also seen to improve with an increase in CF concentration.

The values of the corrosion current density in the absence $(i_{corr,bl})$ and presence of CF extract $(i_{corr,inh})$ were used to estimate the inhibition efficiency from polarization data (IE$_i$%) as follows:

$$\mathrm{IE}_i\% = \left(1 - \frac{i_{corr,inh}}{i_{corr,bl}}\right) \times 100 \tag{4}$$

The obtained values (Table 2), though different from the gravimetric data, however follow the same trend.

Electrochemical Impedance Spectroscopy Data. Impedance studies were undertaken to provide insight into the kinetics of electrode processes at the Fe/1 M HCl and Fe/0.5 M H_2SO_4 interfaces in the absence and presence of CF extract. The impedance responses of these systems are given in Figure 9a and b, respectively, in the Nyquist format. The plots generally comprise of only one depressed capacitive semicircle in the high frequency region, typical for solid metal electrodes that show frequency dispersion of the impedance data.[32,34,35] The transfer function, which can be represented by a solution resistance R_s, shorted by a capacitor (C) that is placed in parallel to the charge transfer resistance R_{ct} (eq 5), where R_s corresponds to the high frequency intercept of the Nyquist


Figure 7. Arrhenius plots for low carbon steel corrosion in (a) 1 M HCl and (b) 0.5 M H_2SO_4 without and with CF extract.

Figure 8. Potentiodynamic polarization curves of low carbon steel in (a) 1 M HCl and (b) 0.5 M H$_2$SO$_4$ solution without and with CF extract.

Table 2. Electrochemical Data for Low Carbon Steel in 1 M HCl and 0.5 M H$_2$SO$_4$ without and with CF Extract

system	E_{corr} (mV) vs SCE	i_{corr} (μA/cm^2)	IE$_i$ (%)	R_{ct} (Ωcm^2)	C_{dl} (μFcm^{-2})	IE$_R$%
1.0 M HCl	−521.6	888.7		94.03	77.09	
200 mg/L CF	−485.6	203.4	77.1	384.7	53.5	75.6
1000 mg/L CF	−490.7	86.5	90.3	651.4	39.8	85.6
0.5 M H$_2$SO$_4$	−482.3	1534.9		63.1	51.2	
200 mg/L CF	−480.8	226.5	85.2	308.2	40.8	79.8
1000 mg/L CF	−475.7	62.3	95.9	912.7	35.3	93.1

semicircle with the real axis while the low frequency intercept with the real axis ascribed to R_{ct}.
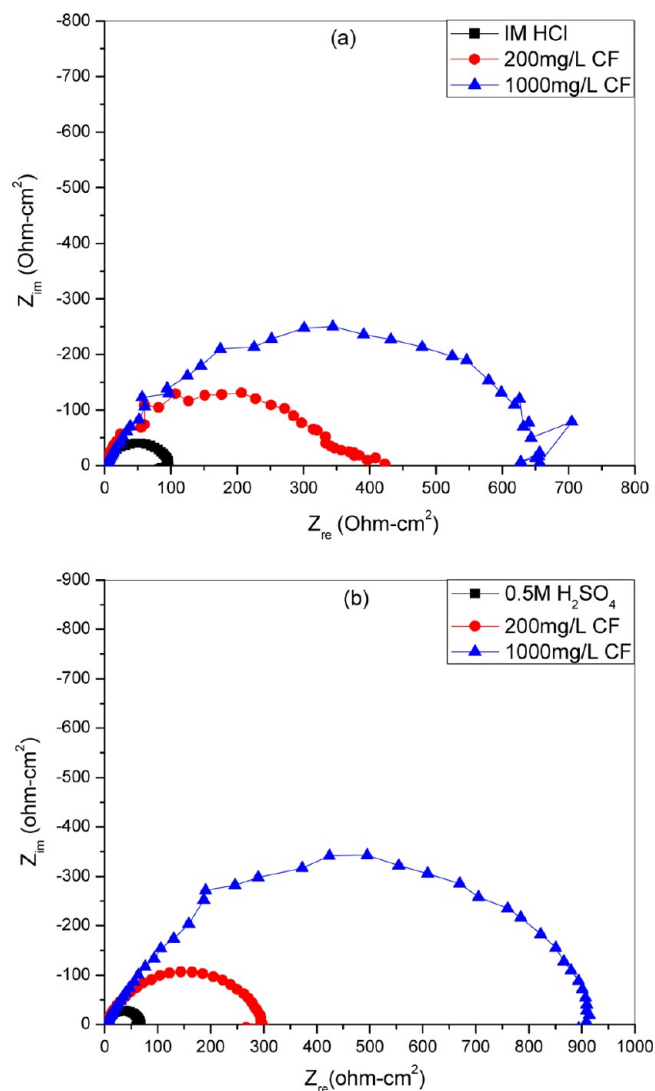
Figure 9. Electrochemical impedance spectra of low carbon steel in (a) 1 M HCl solution and (b) 0.5 M H$_2$SO$_4$ without and with CF extract.

$$Z_{(\omega)} = R_s + \left(\frac{1}{R_{ct}} + j\omega C \right)^{-1} \tag{5}$$

Equation 5 cannot account for the depression of the capacitive semicircle as it is only applicable for homogeneous systems. However, replacing the capacitor with a constant phase element (CPE) could compensate for the nonideal frequency response and the resulting nonideal dielectric behavior. The impedance, Z, of the CPE is given by

$$Z_{CPE} = Q_{dl}^{-1}(j\omega)^{-n} \tag{6}$$

where Q_{dl} and n stand for the CPE constant and exponent, respectively, $j = (-1)^{1/2}$ is an imaginary number, and ω is the angular frequency in radians per second, $\omega = 2\pi f$ where f is the frequency in hertz.

The impedance spectra for the Nyquist plots were thus appropriately analyzed by fitting to the equivalent circuit model $R_s(Q_{dl}R_{ct})$, which has been previously used to model the Fe/acid interface.[36,37] The impedance parameters presented in Table 2 reveal that CF extract increased the magnitude of R_{ct} and decreased the Q_{dl} values. The former effect, which corresponds to an increase in the diameter of the Nyquist

semicircle, is due to the corrosion inhibiting efficacy of the extract. The observed decrease in C_{dl} values, which normally results from a decrease in the dielectric constant and/or an increase in the double-layer thickness, often results from substitution of preadsorbed water molecules on the metal/electrolyte interface by adsorbed organics (with lower dielectric constant).

$$Org_{(sol)} + xH_2O_{(ads)} \rightarrow Org_{(ads)} + xH_2O_{(sol)} \qquad (7)$$
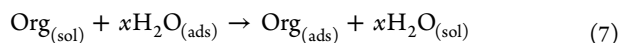
This phenomenon, which provides direct experimental evidence that organic constituents of CF extract are adsorbed on and modify the metal/electrolyte interface (as suggested by the data fit to the Langmuir isotherm) can be linked to the Helmholtz equation:

$$C_{dl} = \varepsilon\varepsilon_o A/\delta \qquad (8)$$

C_{dl} is the double layer capacitance, ε is the dielectric constant of the medium, ε_o the vacuum permittivity, A the electrode area, and δ the thickness of the electrical double layer.

Inhibition efficiency from the impedance data (IE$_R$%) was estimated by comparing the values of the charge transfer resistance in the absence ($R_{ct,bl}$) and presence of inhibitor ($R_{ct,inh}$) as follows:

$$IE_R\% = \left(\frac{R_{ct(inh)} - R_{ct}}{R_{ct(inh)}}\right) \times 100 \qquad (9)$$

The calculated values presented in Table 2 follow the same trend as those from the gravimetric and polarization results.

Computational Studies. Quantum Chemical Calculations. Our experimental results so far show that the corrosion-inhibiting action of CF extract results from adsorption of the organic matter on the corroding mild steel surface. Previous studies have shown that alkaloids play a major role in the adsorption and corrosion inhibiting action of biomass extracts.[38,39] Since metal/inhibitor interactions can be theoretically investigated at the molecular level using computer simulations of suitable models in the framework of the density functional theory (DFT). We thus performed such computations to model the electronic and adsorption structures of the main capsaicinoids present in CF extract; capsaicin and dihydrocapsaisin (Figure 1). The motivation for the computational study is to give a theoretical framework in which to recognize and appreciate the relative contributions of different extract components vis-à-vis their individual adsorption mechanisms and adsorption strengths and not necessarily to provide in depth explanation of the adsorption of the extract.

Quantum chemical computations were performed by means of the DFT electronic structure program DMol[3] using a Mulliken population analysis.[40−43] Electronic parameters for the simulation include restricted spin polarization using the DND basis set and the Perdew−Wang (PW) local correlation density functional. Geometry optimization was achieved using COMPASS force field and the Smart minimize method by high-convergence criteria. This was followed by modeling the electronic structures of the molecules, including the distribution of frontier orbitals and Fukui indices in order to establish the active sites as well as the local reactivity of the molecules. The highest occupied molecular orbital (HOMO), lowest unoccupied molecular orbital (LUMO), and Fukui functions as well as the total electron density of capsaicin and dihydrocapsaisin are presented in Figures 10 and 11, respectively, while Table 3 provides some quantum-chemical parameters related to the
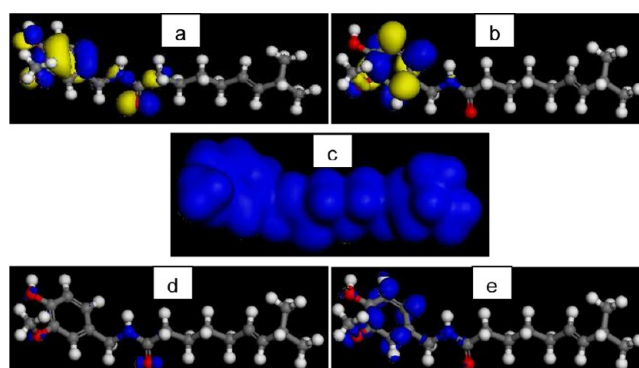
Figure 10. Electronic properties of capsaicin (a) HOMO orbital; (b) LUMO orbital; (c) total electron density; (d) Fukui (f$^-$)function; (e) Fukui (f$^+$) function. The blue and yellow isosurfaces depict the electron density difference; the blue regions show electron accumulation while the yellow regions show electron loss.
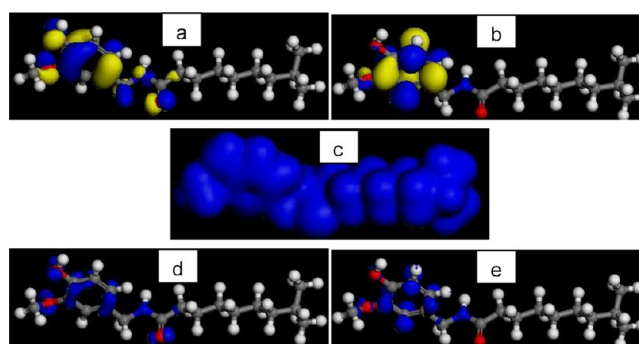
Figure 11. Electronic properties of dihydrocapsaicin (a) HOMO orbital; (b) LUMO orbital; (c) total electron density; (d) Fukui (f$^-$)function; (e) Fukui (f$^+$) function. The blue and yellow isosurfaces depict the electron density difference; the blue regions show electron accumulation while the yellow regions show electron loss.

Table 3. Calculated Quantum Chemical Properties for the Most Stable Conformation of Selected Phytochemical Constituents of CF Extract

property	capsaicin	dihydrocapsaicin
E_{HOMO} (eV)	−5.34	−5.12
E_{LUMO} (eV)	−1.21	−1.04
$E_{LUMO-HOMO}$	4.13	4.08
f_{max}^-	1.33	0.087
f_{max}^+	0.099	0.128

molecular electronic structure of the most stable conformation of the molecules. The electronic distributions of both molecules appear somewhat identical, which is not unexpected since their molecular structures are alike (the only difference being the absence of a double bond in the nonenamide side chain of dihydrocapsaisin).

The HOMO regions for either molecule, which are the sites at which electrophiles attack and represent the active centers with the utmost ability to interact with the metal surface atoms, has contributions from both the methoxyphenol ring and the amide function in the nonenamide chain. On the other hand, the LUMO orbital can accept electrons from the metal using antibonding orbitals to form feedback bonds are saturated around the methoxyphenol ring. Correspondingly, a high value of the HOMO energy (E_{HOMO}) indicates the tendency of a molecule to donate electrons to an appropriate acceptor

molecule with low energy or an empty electron orbital, whereas the energy of the LUMO characterizes the susceptibility of molecules toward nucleophilic attack. Low values of the energy of the gap $\Delta E = E_{LUMO-HOMO}$ implies that the energy to remove an electron from the last occupied orbital will be minimized, corresponding to improved inhibition efficiencies.[44−48] As anticipated from the similarities in electronic structures, E_{HOMO} values (Table 3) do not vary very significantly for capsaicin and dihydrocapsaisin, which means that any observed differences in their adsorption strengths would result from molecular size parameters rather than electronic structure parameters. The seemingly high values of ΔE (>4 eV) are in accordance with the nonspecific nature of the interactions of the molecules with the metal surface.

The local reactivity of each molecule was analyzed by means of the Fukui indices (FI) to assess reactive regions in terms of nucleophilic (f^+) and electrophilic (f^-) behavior. Figures 10d and 11d show that the f^- functions of both molecules correspond with the HOMO locations, indicating the sites through which the molecules could be adsorbed on the metal surface, whereas f^+ (Figures 10e and 11e) correspond with the LUMO locations, showing sites through which the molecules could interact with the nonbonding electrons in the metal. High f^- values are associated with the O atoms of the methoxy and amide functions for both molecules, whereas C atoms of the phenyl ring in α-positions to the methoxy and hydroxyl functions possess high f^+ values. The electron density (charge distribution) is saturated all around each molecule; hence we should expect flat-lying adsorption orientations.

Molecular Dynamics Simulations. Molecular dynamics (MD) simulation of the interaction between single molecules of capsaicin and dihydrocapsaisin and the Fe surface was performed using Forcite quench molecular dynamics in the MS Modeling 4.0 software to sample many different low energy configurations and identify the low energy minima.[49−51] The model metal surface comprised of a Fe crystal cleaved along the (110) plane, with a vacuum layer of 20 Å height on the topside. The geometry of the bottom layer of the slab was constrained to the bulk positions whereas other degrees of freedom were relaxed before optimizing the Fe (110) surface, which was subsequently enlarged into a 16 × 12 supercell. Geometry optimized structures of capsaicin and dihydrocapsaisin were used as adsorbate, which were adsorbed on one side of the Fe (110) slab. Calculations were carried out using the COMPASS force field and the Smart algorithm. The temperature was fixed at 303 K, with the *NVE* (microcanonical) ensemble, with a time step of 1 fs and simulation time 5 ps. The system was quenched every 250 steps.

The lowest energy adsorption models for capsaicin and dihydrocapsaisin on the Fe(110) surface from our simulation are shown in Figures 12 and 13. The molecules can be seen to maintain a flat-lying adsorption orientation on the Fe surface as predicted from the delocalization of the electron density. This orientation maximizes contact and, hence, augments the degree of surface coverage. Quantitative appraisal of the interaction between each molecule and the Fe surface was achieved by calculating the adsorption energy (E_{ads}) using the following equation:

$$E_{Bind} = E_{total} - (E_{Mol} + E_{Fe}) \qquad (10)$$

E_{mol}, E_{Fe}, and E_{total} correspond respectively to the total energies of the molecule, Fe(110) slab, and the adsorbed Mol/Fe (110) couple. In each case the potential energies were calculated by
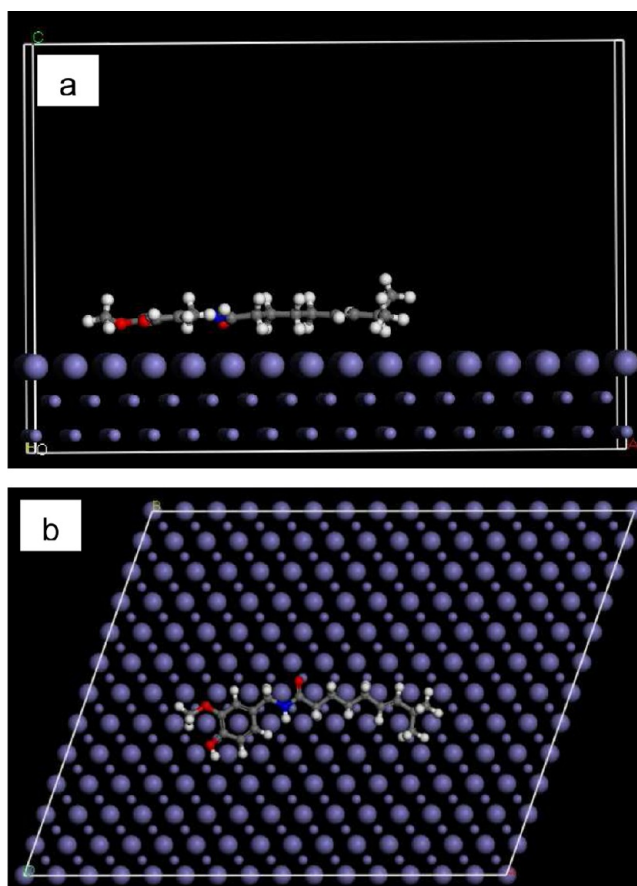
Figure 12. Representative snapshots of capsaicin on Fe(110) (a) side view and (b) on-top view emphasizing the soft epitaxial adsorption mechanism with accommodation of the molecular backbone in characteristic epitaxial grooves on the metal surface (binding energy = −207 kcal/mol).

averaging the energies of the five structures of lowest energy and a negative value of E_{ads} corresponds to a stable adsorption structure. The obtained values of E_{ads} (−207 and −206.4 kcal/mol for capsaicin and dihydrocapsaisin, respectively) are of the same magnitude, which means that both molecules exert comparable contributions to the observed corrosion inhibiting effect of CF extract. More importantly however is the large negative values of the computed adsorption energies, which is more exothermic than expected for non covalent interactions. This probably results from significant dispersive interactions arising from the high polarizability of the O and N atoms, including the π electron delocalization within the phenyl ring, which should enhance adsorption of the molecules.[52] Moreover, close inspection of the on-top view of the molecules adsorbed on Fe(110) reveals a very clear trend in the adsorption configuration of both molecules wherein polarizable atoms along the molecular backbone as well as the phenyl ring align with vacant sites on the fcc lattice atop the metal surface and actually avoid contact with the Fe atoms on the surface plane (larger spheres on the Fe slab). This corresponds to accommodation of the molecular backbone in characteristic epitaxial grooves on the metal surface. Epitaxial adsorption orientations have been reported for noncovalent adsorption of amino acids[53,54] as well as phytochemical constituents of certain biomass extracts on metal surfaces.[55] Such orientations are associated with a minimum free energy of adsorption as the

221

dx.doi.org/10.1021/sc300145k | *ACS Sustainable Chem. Eng.* 2013, 1, 214−225
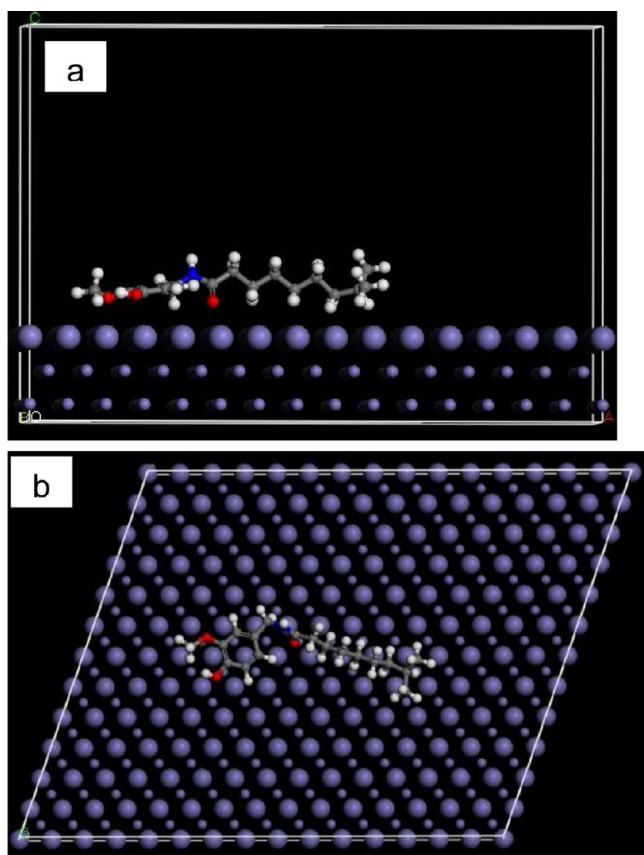
Figure 13. Representative snapshots of dihydrocapsaicin on Fe(110) (a) side view and (b) on-top view emphasizing the soft epitaxial adsorption mechanism with accommodation of the molecular backbone in characteristic epitaxial grooves on the metal surface (binding energy = −206.4 kcal/mol).

adsorbed molecules can be considered as extensions of the fcc lattice and adsorption strength scales with improved fit of the polarizable atoms of a molecule to multiple epitaxial sites. This phenomenon accounts for the obtained high binding energies of the phytochemical constituents of CF, hence the remarkable corrosion inhibiting effect of the extract as observed experimentally.

Antimicrobial Activity. Microbial growth on metals and alloys of industrial usage affect the performance of exposed metal parts in different ways. The most corrosion-relevant microbes cited in many corrosion problems are the sulfate-reducing bacteria, which can transform sulfate into sulfide, thus having a deteriorative effect on metal surfaces.[13,14] Interestingly, extracts of pepper plants contain several phytochemical compounds with proven antimicrobial activity. For instance, aqueous extracts from the fruits of *Capsicum frutescens* have been reported to exhibit antimicrobial action against *Bacillus cereus, Bacillus subtilis, Clostridium sporogenes, Clostridium tetani,* and *Streptococcus pyogenes, Vibrio cholerae, Staphylococcus aureus,* and *Salmonella typhimurium*.[56−59] Again, saponins isolated from CF, including CAY-1, have been reported to possess fungicidal activity against *Candida albicans, Aspergillus* spp, *Fusarium* spp, *Trichophyton* spp. and *Microsporum* spp.[60] Accordingly, the established efficacy of biomass extracts on pathogenic microorganisms could be further exploited for the control of corrosion-associated microorganisms.

The ability of the crude extracts of *Capsicum frutescens* to inhibit microbial growth was investigated in experiments employing the sulfate reducing bacteria *Desulfotomaculum* sp. The results of the biocidal activity tests are shown in Figures 14
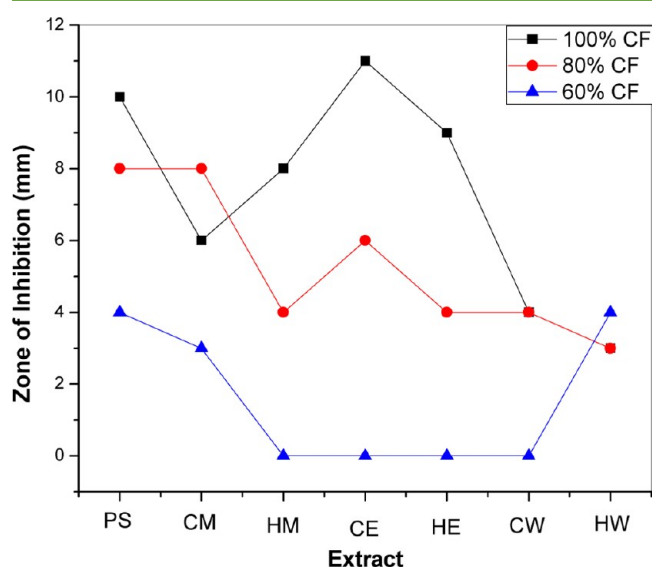
Figure 14. Antibacterial activity (zone of growth inhibition) of different extracts of *Capsicum frutescens* (CF) against *Desulfotomaculum* species (PS = petroleum spirit, CM = cold methanol, HM = hot methanol, CE = cold ethanol, HE = hot ethanol, CW = cold water, HW = hot water).
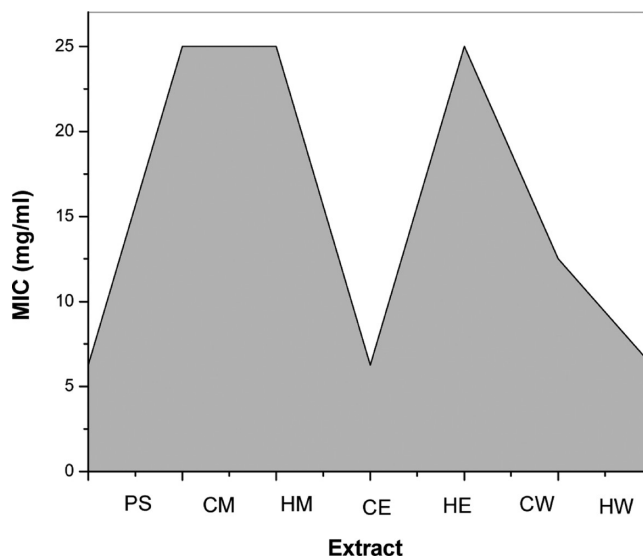
Figure 15. Minimum inhibitory concentration (MIC) of different extracts of *Capsicum frutescens* (CF) on *Desulfotomaculum* species (PS = petroleum spirit, CM = cold methanol, HM = hot methanol, CE = cold ethanol, HE = hot ethanol, CW = cold water, HW = hot water).

and 15. The relative antibacterial activity of the extracts is reflected by the mean zones of bacteria growth inhibition. The highest growth inhibitory activity was obtained from the stock solutions of the extracts, with the cold ethanol (CE) and petroleum spirit (PS) extracts showing higher efficacy. The inhibiting effect generally decreased as the extracts were diluted

with distilled water and most of the extracts became ineffective at about 60% dilution. Figure 15 depicts the minimum inhibitory concentration (MIC) of the extracts. Generally, the MIC follow the same trend as the growth inhibiting effect of the extracts, with the ethanol, petroleum spirit, and hot water extracts requiring lower concentrations (6.25 mg/mL) to initiate biocidal action on *Desulfotomaculum* species, followed by the cold water extract (12.5 mg/mL), while the cold methanol, hot methanol, and hot ethanol extracts had MICs of 25 mg/mL.

Although the detailed mechanism of the biocidal action of CF extract was not extensively investigated in this study, the observed growth inhibition of *Desulfotomaculum* species, as with all other reported cases of its antimicrobial efficacy, could be attributed mainly to the pungent capsaicinoid constituents therein.[61] Additional contributions can also come from the lipids-dissolving ability of the saponin moeties, which results in loss of cellular content as well as the protein binding abilities of tannins, which facilitates interferes with key metabolic functions of the cells.[62]

Studies have shown that corrosion mostly occurred while biofilms are being established, which is often prior to the addition of biocides.[14] Again, it is well-known that mature biofilms are far more resistant to biocides than bacterial cells in solution. As corrosion inhibiting formulations are often introduced at inception of any process, it should be very advantageous that the corrosion inhibitors possess some biocidal activity in order to hinder biofilm formation early enough. The general idea is to regulate the environment ab initio, making it unfavorable for biofilm formation and growth as well as protecting the metal from corrosion. The use of CF extracts in corrosion inhibitor formulations ensures such simultaneous control of corrosion and biofilm formation. Moreover, the individual biocidal activities of the different phytochemical constituents could alter the nature of the biofilm or disrupt the metabolism of some of the major microbial groups present in the biofilm, thereby limiting the associated corrosion damage without necessarily attempting to kill all microorganisms. The use of biomass extracts ensures that all these features are achieved using additives that are inexpensive, readily available, nontoxic, and biodegradable.

Caution!: Pure capsaicin is of course an irritant for mammals, including humans, and produces a sensation of burning in any tissue with which it comes into contact. Accordingly, it must be handled with care, avoiding inhalation of its particles and preventing its contact with any part of the body. Severe overexposure to pure capsaicin can result in death; the lethal dose (LD_{50} in mice) is 47.2 mg/kg.[63] However, such doses can rarely be encountered from handling the aqueous extract of CF.

CONCLUSIONS

Capsicum frutescens extract inhibited the acid corrosion of low carbon steel as well as the growth of the gram positive sulfate reducing bacteria, *Desulfotomaculum* species. Polarization measurements show that the corrosion inhibition proceeded via mixed-type mechanism, which the impedance data indicate was achieved via adsorption of organic constituents of the extract on the carbon steel surface. DFT-based quantum chemical computations of parameters associated with the molecular electronic structures of the active alkaloidal constituents of the extract (capsaicin and dihydrocapsaicin) confirmed their corrosion inhibiting potential and established their individual contributions to the observed inhibiting effect.

The noncovalent adsorption geometries of both molecules on Fe show clear evidence of soft epitaxial adsorption and the magnitude of the physisorption energies agree more or less with the remarkable trend of experimentally determined inhibition efficiencies.

CF extracts also exhibited high inhibitory activity on the growth of the SRB (*Desulfotomaculum* sp.), with the effect of the ethanol and petroleum spirit extracts being more pronounced than those of the methanol and water extracts. The antimicrobial effect of the extract is attributable to the phytochemical constituents of the (alkaloids, tannins, saponins), which disrupt the growth and essential metabolic functions of the bacteria.

The results obtained in this project support our hypothesis that the complex phytochemical composition of biomass extracts could be exploited for the simultaneous control of chemical and microbial influenced corrosion of metals and alloys.

AUTHOR INFORMATION

Corresponding Author

*E-mail: oguziemeka@yahoo.com; emekaoguzie@gmail.com. Tel.: +2348037026581.

Notes

The authors declare no competing financial interest.

REFERENCES

(1) Majjane, A.; Rair, D.; Chahine, A.; Et-tabirou, M.; Ebn Touhami, M.; Touir, R. Preparation and characterization of a new glass system inhibitor for mild steel corrosion in hydrochloric solution. *Corros. Sci.* **2012**, *60*, 98−103.

(2) Pavithra, M. K.; Venkatesha, T. V.; Punith Kumar, M. K.; Tondan, H. C. Inhibition of mild steel corrosion by Rabeprazole sulfide. *Corros. Sci.* **2012**, *60*, 104−111.

(3) Tao, Z.; He, W.; Wang, S.; Zhang, S.; Zhou, G. A study of differential polarization curves and thermodynamic properties for mild steel in acidic solution with nitrophenyltriazole derivative. *Corros. Sci.* **2012**, *60*, 205−213.

(4) Singh, A. K.; Shukla, S. K.; Quraishi, M. A.; Ebenso, E. E. Investigation of adsorption characteristics of N,N'-[(methylimino)-dimethylidyne]di-2,4-xylidine as corrosion inhibitor at mild steel/sulphuric acid interface. *J. Taiwan Inst. Chem. Eng.* **2012**, *43*, 463−472.

(5) Zhao, J.; Chen, G. The synergistic inhibition effect of oleic-based imidazoline and sodium benzoate on mild steel corrosion in a CO₂-saturated brine solution. *Electrochim. Acta* **2012**, *69*, 247−255.

(6) Yüce, A. O.; Kardaş, G. Adsorption and inhibition effect of 2-thiohydantoin on mild steel corrosion in 0.1M HCl. *Corros. Sci.* **2012**, *58*, 86−94.

(7) Wang, X.; Yang, H.; Wang, F. An investigation of benzimidazole derivative as corrosion inhibitor for mild steel in different concentration HCl solutions. *Corros. Sci.* **2011**, *53*, 113−121.

(8) Bahrami, M. J.; Hosseini, S. M. A.; Pilvar, P. Experimental and theoretical investigation of organic compounds as inhibitors for mild

223

dx.doi.org/10.1021/sc300145k | ACS Sustainable Chem. Eng. 2013, 1, 214−225

steel corrosion in sulfuric acid medium. *Corros. Sci.* **2010**, *52*, 2793−2803.

(9) Shibli, S. M. A.; Saji, V. S. Co-inhibition characteristics of sodium tungstate with potassium iodate on mild steel corrosion. *Corros. Sci.* **2005**, *47*, 2213−2224.

(10) Shibli, S. M. A.; Saji, V. S. The effect of neutral red on the corrosion inhibition of cold rolled steel in 1.0 M hydrochloric acid. *Corros. Sci.* **2005**, *47*, 2213−2224.

(11) Hernández Gayosso, M. J.; Zavala Olivares, G.; Ruiz Ordaz, N.; Juárez Ramirez, C.; Garcia Esquivel, R.; Padilla Viveros, A. Microbial consortium influence upon steel corrosion rate, using polarisation resistance and electrochemical noise techniques. *Electrochim. Acta* **2004**, *49*, 4295−4301.

(12) Fang, H. H. P.; Xu, L.-C.; Chan, K.-Y. Effects of toxic metals and chemicals on biofilm and biocorrosion. *Water Res.* **2002**, *36*, 4709−4716.

(13) Videla, H. A.; Herrera, L. K. Microbiologically influenced corrosion: looking to the future. *Int. Microbiol.* **2005**, *8*, 169−180.

(14) Angell, P.; Urbanic, K. Sulphate-reducing bacterial activity as a parameter to predict localized corrosion of stainless alloys. *Corros. Sci.* **2000**, *42*, 897−912.

(15) Ismail, Kh.M.; Jayaraman, A.; Wood, T. K.; Earthman, J. C. The influence of bacteria on the passive film stability of 304 stainless steel. *Electrochim. Acta* **1999**, *44*, 4685−4692.

(16) Flemming, H. C. Economical and technical overview. In *Microbially influenced corrosion of materials*; Heitz, E., Flemming, H. C., Sand, W., Eds.; Springer-Verlag: Berlin, Heidelberg, 1996.

(17) Li, J.; Yao, C.; Liu, Y.; Li, D.; Zhou, B.; Cai, W. The hazardous hexavalent chromium formed on trivalent chromium conversion coating: The origin, influence factors and control measures. *J. Haz. Mater.* **2012**, *221−222*, 56−61.

(18) Barrera-Díaz, C. E.; Lugo-Lugo, V.; Bilyeu, B. A review of chemical, electrochemical and biological methods for aqueous Cr(VI) reduction. *J. Haz. Mater.* **2012**, *223−224*, 1−12.

(19) Behpour, M.; Ghoreishi, S. M.; Khayatkashani, M.; Soltani, N. The effect of two oleo-gum resin exudate from Ferula assa-foetida and Dorema ammoniacum on mild steel corrosion in acidic media. *Corros. Sci.* **2011**, *53*, 2489−2501.

(20) Garai, S.; Garai, S.; Jaisankar, P.; Singh, J. K.; Elango, A. A comprehensive study on crude methanolic extract of Artemisia pallens (Asteraceae) and its active component as effective corrosion inhibitors of mild steel in acid solution. *Corros. Sci.* **2012**, *60*, 193−204.

(21) Oguzie, E. E. Evaluation of the inhibitive effect of some plant extracts on the acid corrosion of mild steel. *Corros. Sci.* **2008**, *50*, 2993−2998.

(22) Rosliza, R.; Wan Nik, W. B. Improvement of corrosion resistance of AA6061 alloy by tapioca starch in sea water. *Curr. Appl. Phys.* **2010**, *10*, 221−229.

(23) Abiola, O. K.; James, A. O. The effects of Aloe vera extract on corrosion and kinetics of corrosion process of zinc in HCl solution. *Corros. Sci.* **2010**, *52*, 661−664.

(24) Oguzie, E. E.; Onuchukwu, A. I. Inhibition of mild steel corrosion in acidic media by aqueous extracts from Garcinia kola seeds. *Corros. Rev.* **2007**, *25*, 355−362.

(25) Ostovari, A.; CHoseinieh, S. M.; Peikari, M.; Shadizadeh, S. R.; Hashemi, S. J. Corrosion inhibition of mild steel in 1M HCl solution by henna extract: A comparative study of the inhibition by henna and its constituents (Lawsone, Gallicacid, a-D-Glucose and Tannicacid). *Corros. Sci.* **2009**, *51*, 1935−1949.

(26) Satapathy, A. K.; Gunasekaran, G.; Sahoo, S. C.; Amit, K.; Rodrigues, P. V. Corrosion inhibition by Justicia gendarussa plant extract in hydrochloric acid solution. *Corros. Sci.* **2009**, *51*, 2848−2856.

(27) Okwu, D. E.; Josiah., C. Evaluation of the chemical composition of two Nigerian medicinal plant. *Afri. J. Biotechnol.* **2006**, *5*, 357−361.

(28) Okoli, C. O.; Akah, P. A.; Nwafor, S. V.; Anisiobi, A. I.; Ibegbunam, I. N.; Erojikwe, O. Anti-inflammatory activity of hexane leaf extract of *Aspilia africana* C.D. Adams. *J. Ethnopharmacol.* **2007**, *109*, 219−225.

(29) Harbone, J. D. *Phytochemical Methods*; Chapman and Hall: London, 1998.

(30) Tolan, I.; Ragoobirsingh, D.; Morrison, E. Y. Isolation and purification of the hypoglycaemic principle present in *Capsicum frutescens*. *Phytother. Res.* **2004**, *18*, 95−96.

(31) Luning, P. A.; de Rijk, T.; Wichers, H. J.; Roozen, J. P. Gas chromatography, mass spectrometry, and sniffing port analyses of volatile compounds of fresh bell peppers (*Capsicum annuum*) at different ripening stages. *J. Agric. Food Chem.* **1994**, *42*, 977−983.

(32) Ashassi-Sorkhabi, H.; Seifzadeh, D.; Hosseini, M. G. EN, EIS and polarization studies to evaluate the inhibition effect of 3H-phenothiazin-3-one, 7-dimethylamin on mild steel corrosion in 1M HCl solution. *Corros. Sci.* **2008**, *50*, 3363−3370.

(33) Martinez, S. Inhibitory mechanism of mimosa tannin using molecular modeling and substitutional adsorption isotherms. *Mater. Chem. Phys.* **2003**, *77*, 97−102.

(34) Khaled, K. F. Electrochemical investigation and modeling of corrosion inhibition of aluminum in molar nitric acid using some sulphur-containing amines. *Corros. Sci.* **2010**, *52*, 2905−2916.

(35) Popova, A.; Sokolova, E.; Raicheva, S.; Christov, M. AC and DC study of the temperature effect on mild steel corrosion in acid media in the presence of benzimidazole derivatives. *Corros. Sci.* **2003**, *45*, 33−58.

(36) Oguzie, E. E.; Wang, S. G.; Li, Y.; Wang, F. H. Influence of iron microstructure on corrosion inhibitor performance in acidic media. *J. Phy. Chem. C* **2009**, *113*, 8420−8429.

(37) Oguzie, E. E.; Li, Y.; Wang, F. H. Corrosion inhibition and adsorption behaviour of methionine on mild steel in sulphuric acid and synergistic effect of iodide ion. *J. Colloid Interface Sci.* **2007**, *310*, 90−98.

(38) Oguzie, E. E.; Ogukwe, C. E.; Ogbulie, J. N.; Nwanebo, F. C.; Adindu, C. B.; Udeze, I. O.; Oguzie, K. L.; Eze, F. C. Broad spectrum corrosion inhibition: Corrosion and microbial (SRB) growth inhibiting effects of *Piper guineense* extract. *J. Mater. Sci.* **2012**, 3592−3601.

(39) Lecante, A.; Robert, F.; Blandinières, P. A.; Roos, C. Anti-corrosive properties of S. tinctoria and G. ouregou alkaloid extracts on low carbon steel. *Curr. Appl. Phys.* **2011**, *11*, 714−724.

(40) Delley, B. J. An all-electron numerical method for solving the local density functional for polyatomic molecules. *Chem. Phys.* **1990**, *92*, 508−518.

(41) Delley, B. J. From molecules to solids with the Dmol³ approach. *Chem. Phys.* **2000**, *113*, 7756−7765.

(42) Khaled, K. F. Studies of iron corrosion inhibition using chemical, electrochemical and Computer simulation techniques. *Electrochim. Acta* **2010**, *55*, 6523−6532.

(43) Fu, J.; Li, S.; Wang, Y.; Cao, L.; Lu, L. Computational and electrochemical studies of some amino acid compounds as corrosion inhibitors for mild steel in hydrochloric acid solution. *J. Mater. Sci.* **2010**, *45*, 6255−6265.

(44) Gece, G.; Bilgi, S. A theoretical study on the inhibition efficiencies of some amino acids as corrosion inhibitors of nickel. *Corros. Sci.* **2010**, *52*, 3435−3443.

(45) Musa, A. Y.; Jalgham, R. T. T.; Mohamad, A. B. Molecular dynamic and quantum chemical calculations for phthalazine derivatives as corrosion inhibitors of mild steel in 1M HCl. *Corros. Sci.* **2012**, *56*, 176−183.

(46) Özkir, D.; Kayakirilmaz, K.; Bayol, E.; Gürten, A. A.; Kandemirli, F. The inhibition effect of Azure A on mild steel in 1M HCl. A complete study: Adsorption, temperature, duration and quantum chemical aspects. *Corros. Sci.* **2012**, *56*, 143−152.

(47) Bahrami, M. J.; Hosseini, S. M. A.; Pilvar, P. Experimental and theoretical investigation of organic compounds as inhibitors for mild steel corrosion in sulfuric acid medium. *Corros. Sci.* **2010**, *52*, 2793−2803.

(48) Cruz, J.; Pandiyan, T.; García-Ochoa, E. A new inhibitor for mild carbon steel: electrochemical and DFT studies. *J. Electroanal. Chem.* **2005**, *583*, 8−16.

(49) Casewit, C. J.; Colwell, K. S.; Rappé, A. K. Application of universal force field to organic molecules. *J. Am. Chem. Soc.* **1992**, *114*, 10035−10046.

(50) Casewit, C. J.; Colwell, K. S.; Rappé, A. K. Application of universal force field to main group elements. *J. Am. Chem. Soc.* **1992**, *114*, 10046−10053.

(51) Oguzie, E. E.; Enenebeaku, C. K.; Akalezi, C. O.; Okoro, S. C.; Ayuk, A. A.; Ejike, E. N. Adsorption and Corrosion inhibiting effect of Dacryodis edulis extract on low carbon steel corrosion in acidic media. *J. Colloid Interface Sci.* **2010**, *349*, 283−292.

(52) Heinz, H.; Farmer, B. L.; Pandey, R. B.; Slocik, J. M.; Patnaik, S. S.; Pachter, R.; Naik, R. R. Nature of molecular interactions of peptides with gold, palladium, and Pd-Au bimetal surfaces in aqueous solution. *J. Am. Chem. Soc.* **2009**, *131*, 9704−9714.

(53) Feng, J.; Pandey, R. B.; Berry, R. J.; Farmer, B. L.; Naik, R. R.; Heinz, H. Adsorption mechanism of single amino acid and surfactant molecules to Au {111} surfaces in aqueous solution: design rules for metal-binding molecules. *Soft Matter* **2011**, DOI: 10.10 39/c0sm01118e.

(54) Oguzie, E. E.; Li, Y.; Wang, S. G.; Wang, F. H. Understanding corrosion inhibition mechanisms − Experimental and theoretical approach. *RSC Adv.* **2011**, *1*, 866−873.

(55) Mejeha, M. I.; Nwandu, M. C.; Okeoma, K. B.; Nnanna, L. A.; Chidiebere, M. A.; Eze, F. C.; Oguzie, E. E. Corrosion inhibition and adsorption behavior of leaf extracts of *Aspilia africana* on aluminium alloy AA 3003 in hydrochloric acid. *J. Mater. Sci.* **2012**, *47*, 2559−2572.

(56) Shariati, A.; Pordeli, H. R.; Khademian, A.; Aydani, M. Evaluation of the antibacterial effects of Capsicum spp. extracts on the multi-resistant Staphylococcus aureus strains. *J. Plant Sci. Res.* **2010**, *5*, 76−83.

(57) De Lucca, A. J.; Boue, S.; Palmgren, M. S.; Maskos, K.; Cleveland, T. E. Fungicidal properties of two saponins from Capsicum frutescens and the relationship of structure and fungicidal activity. *Can. J. Microbiol.* **2006**, *52*, 336−342.

(58) Cichewicz, R. H.; Thorpe, P. A. The antimicrobial properties of chile peppers (Capsicum species) and their uses in Mayan medicine. *Ethnopharmacol.* **1996**, *52*, 61−70.

(59) Koffi-Nevry, R.; Kouassi, K. C.; Nanga, Z. Y.; Koussémon, M.; Loukou, G. Y. Antibacterial Activity of Two Bell Pepper Extracts: *Capsicum annuum* L and *Capsicum frutescens*. *Int. J. Food Prop.* **2012**, 961−971.

(60) Stergiopoulou, T.; De Lucca, A. J.; Meletiadis, J.; Sein, T.; Boue, S. M.; Schaufele, R.; Roilides, E.; Ghannoum, M.; Walsh, T. J. In vitro activity of CAY-1, a saponin from Capsicum frutescens, against Microsporum and Trichophyton species. *Med. Mycol.* **2008**, *46*, 805−810.

(61) Soetarno, S. S.; Yulinah, E.; Sylvia. Antimicrobial Activities of the Ethanol Extracts of Capsicum Fruits with Different Levels of Pungency. *JMS* **1997**, *2*, 57−63.

(62) Wina, E. Saponins: Effects on Rumen Microbial Ecosystem and Metabolism in the Rumen. *Dietary Phytochem. Microbes* **2012**, 311−350.

(63) Johnson, W. Final report on the safety assessment of *Capsicum annuum* extract, *Capsicum annuum* fruit extract, *Capsicum annuum* resin, *Capsicum annuum* fruit powder, *Capsicum frutescens* fruit, *Capsicum frutescens* fruit extract, *Capsicum frutescens* resin, and *Capsaicin*. *Int. J. Toxicol.* **2007**, *26*, 3−106.